Chemosphere 371 (2025) 144082

Contents lists available at ScienceDirect

Chemosphere

journal homepage: www.elsevier.com/locate/chemosphere

Effect of intermittent water flow on biodegradation of organic micropollutants in the hyporheic zone

Maria Vittoria Barbieri [a,*], Oriane Della-Negra [a,b], Dominique Patureau [b], Serge Chiron [a]

[a] HydroSciences Montpellier, University of Montpellier, IRD, CNRS, 15 Av. Charles Flahault, 34090, Montpellier, France
[b] INRAE, Univ Montpellier, LBE, 102 avenue des Étangs, Narbonne, 11100, France

HIGHLIGHTS

- Hyporheic zones in intermittent rivers contribute to organic micropollutant degradation.
- Intermittent flows stimulate the biodegradation of selected organic micropollutants.
- Biodegradation rate enhancements can be ascribed to additional transformation routes.
- Identification of transformation products reveal oxidative and reductive pathways.
- Desiccation periods favor nitrifying/denitrifying bacteria and the degrader *Ralstonia*.

GRAPHICAL ABSTRACT

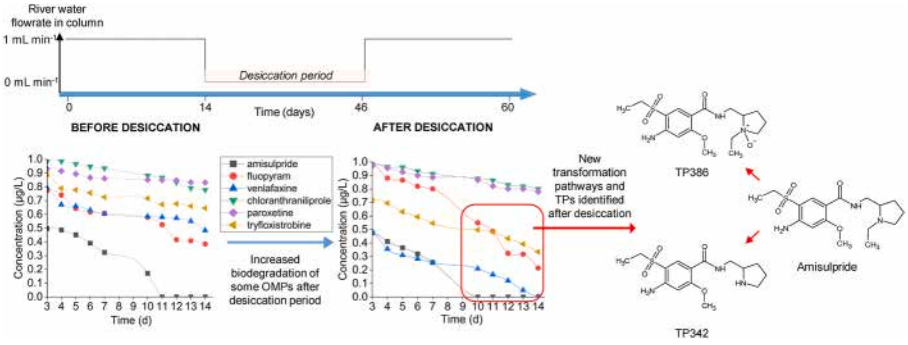

ARTICLE INFO

Handling Editor: T Cutright

Keywords:
Biodegradation
flow intermittency
Organic micropollutants
Reductive pathways
Transformation products

ABSTRACT

Water scarcity in the Mediterranean area has increased the number of intermittent rivers. Recently, hyporheic zones (HZ) of intermittent rivers have gained attention since a substantial part of the stream's natural purification capacity is located within these zones. Thus, understanding the flow dynamics in HZs is crucial for gaining insights into the degradation of organic micropollutants. A lab-scale study using column experiments was conducted in an attempt to elucidate the environmental processes accounting for the biodegradation capacity of the HZ under flow intermittency. A mixture of six compounds including pesticides (chloranthraniliprole, fluopyram and trifloxystrobin) and pharmaceuticals (venlafaxine, amisulpride and paroxetine) spiked at 1 µg/L level was used for degradation kinetic studies and at 1 mg/L for transformation products identification using suspect/non-target liquid chromatography high-resolution mass spectrometry approaches. The experiments lasted 60 days, divided into two 14-day phases: one before and one after a 5-week desiccation period. Bacterial community was charaterized by high-throughput DNA sequencing. The results suggested that intermittent flows stimulated the biodegradation of three compounds namely fluopyram, trifloxystrobin and venlafaxine, showing a large range of biodegradation profiles in batch water/sediment testing system according to OECD 308 tests. Biodegradation rate enhancement was ascribed to the occurrence of additional transformation routes after the desiccation period of river sediment, with the formation of new transformation products reported for the first time in the present work. 16S rDNA sequencing revealed that the desiccation period favored the growth of nitrifying and denitrifying bacteria which could partially explain the emergence of the new transformation pathways and most

* Corresponding author.
E-mail address: mariavittoria.barbieri@idaea.csic.es (M.V. Barbieri).

https://doi.org/10.1016/j.chemosphere.2025.144082
Received 18 October 2024; Received in revised form 2 January 2025; Accepted 4 January 2025
Available online 8 January 2025

specifically those leading to N-oxide derivatives. Identification of transformation products also revealed that reductive transformation routes were relevant for this study, being dehydrogenation, dehalogenation, ether bond cleavage and sulfone reduction into sulphide important reactions. These results suggest that the intermittent flow conditions can influence the HZ biodegradation capacity.

1. Introduction

Limiting water pollution is crucial for meeting the UN Sustainable Development Goals. Nature-based solutions such as river restoration can be relevant for this purpose, and central in the context of aquatic health is the hyporheic zone (HZ) (Popp et al., 2024). The HZ is the upper zone of the streambed where exchanges between shallow groundwater and surface water occur. In natural streams, HZ acts as a natural hydrodynamically-driven bioreactor with attenuation capacities not only of nutrients and dissolved organic matter (DOM) but also of organic micropollutants (OMP) (Perata-Maraver et al., 2018). HZs significantly contribute to OMP self-purification of streams and increase their overall water quality (Schaper et al., 2018). OMP attenuation rates have shown temporal variability in terms of residence time which may increase the growth of microbial community and account for faster OMP degradation (Posselt et al., 2020). OMP attenuation has found to be dependent on redox conditions (Rutere et al., 2021) and on the availability of biodegradable DOM, appointing to analogous transformation pathways for both OMP and DOM (Mueller et al., 2021). The most elevated removal rates of OMP occur in the shallow HZ, characterized by the highest carbon turnover rates and oxic redox conditions (Schaper et al., 2019). However, the intensity of hyporheic exchange as well as microbial diversity have been found to be the main drivers to promote in-stream OMP reactivity (Betterle et al., 2021). These microbially-mediated transformations were made possible because a large surface area is provided for the microbial communities for the formation of biofilms in sediments. Biodegradation has been considered even more efficient in HZ than in activated sludge processes, since longer residence time increases the adaptation of microbial community and its diversity, accounting for higher rates of metabolic pathways (Posselt et al., 2020).

Links between pollutant reactivity and microbial processes have recently been established using multi-fluorescent tracer experiments (Höhne et al., 2022). However, all these studies were mainly conducted in urban perennial rivers, where mainly pharmaceutical residues originating from WWTP occur and a high variability in OMP half-lives have been observed due to the diversity and complexity of real-world conditions. Batch and column experiments (Borreca et al., 2024; Burke et al., 2014) dealing with the chemical processes occurring in the hyporheic zones have been conducted recently, as well as first approaches of field-based studies dealing with the heterogeneity of field conditions (Reith et al., 2023). In addition, only a few of those studies have dealt with the formation of transformation products (TPs) (Peter et al., 2019; Posselt et al., 2020; Sabater-Liesa et al., 2021).

A special case is undoubtedly intermittent streams where HZ can remain dry for weeks or even months. In intermittent rivers, flow temporally stops at specific locations along the river. In Mediterranean area, the dry season can last several months and during that time, insufficient dilution of the pollutants is a major issue, influencing river ecology. The duration of the dry season depends on the country, but it generally ranges from June to September in most countries and specifically in France.These environmental settings have been poorly investigated for OMP attenuation, despite the critical importance of gaining a deeper understanding of HZ to enhance their functionality in reducing OMP. What is known is that bacteria living in sediments may respond faster to desiccation due to their short life-cycle. This induces changes in reducing bacterial diversity by pushing the structure of river bacterial communities towards those present in soils (Romero et al., 2019). Interestingly, in rivers submitted to strong hydrological stress, an increased water hydrologic travel time accounting for higher attenuation rates of most OMP of the present work has been observed (Mandaric et al., 2019). In certain instances, intermittent water flow may encourage the temporary breakdown of pharmaceuticals known for their limited biodegradability (Rosman et al., 2018). This discovery implies that the presence of pharmaceuticals in aquatic environments experiencing hydrological disruptions might sustain their biodegradation capacity. This warrants further exploration, as it holds significance for enhancing our comprehension of intermittent aquatic ecosystems.

The main contribution of the work was therefore to investigate the effects of HZ desiccation on OMP degradation including selected pesticides and pharmaceuticals, chosen for this study due to their different accumulation and bioaccumulation potential, their toxicity to non-target organisms including mammals and fish, and to their occurrence in the river areas where sediments were collected.

Specific objectives included investigating the overall effects of desiccation on i) OMP degradation kinetics, ii) OMP transformation pathways following TPs identification by applying suspect and non-target screening based on liquid chromatography-high resolution mass spectrometry (LC-HRMS) approaches and iii) the overall effects of desiccation on HZ bacterial community composition by time-resolved high-throughput DNA sequence analysis. Column experiments were employed in laboratory studies because, despite the fact that mesocosm experiments may not consistently capture natural systems accurately, they play a crucial role in yielding valuable data regarding observable effects at the ecosystem level, all within a reasonable cost (Banzhaf and Hebig, 2016).

2. Material and methods

2.1. Chemicals

Analytical standards for the target compounds (amisulpride, chlorantraniliprole, fluopyram, trifloxystrobin, venlafaxine) and their deuterated analogues, as well as amisulpride-N-oxide, venlafaxine-N-oxide, N-desmethylvenlafaxine, and O-desmethylvenlafaxine, were procured from Toronto Research Chemicals (Toronto, Canada). Paroxetine and formic acid (FA) (puriss p.a. ACS reagent analytical grade) were acquired from Sigma Aldrich (St Quentin-Fallavier, France).

Compounds were selected on the basis of their ng/L occurrence at the wastewater-impacted river location where sediments were collected. The selected OMPs encompassed a wide range of physico-chemical properties with diverse solubility (log P ranging from 0.9 to 4.5) and dissipation behaviors, from fast degrading to persistent in water/sediment system with DT_{50} in the 1.8–1000 days range (see Table S1). Antidepressants including venlafaxine, amisulpride and paroxetine were selected for this work because the primary targets for bioaccumulable antidepressants action has shown high structural conservation between mammals and fish with suspected effects on wild fish populations (Gould et al., 2021). Venlafaxine and amisulpride are biodegradable compounds in OECD 308 type aerobic water/sediment testing systems (Manasfi et al., 2022), while paroxetine was found persistent in aerobic biodegradation studies (Cunnigham et al., 2004). All these compounds are cationic compounds with a potential sorption capacity on sediment. Fluopyram, a potent inhibitor of succinate dehydrogenase inhibitor (SDHI) in fungi and nematodes (Schleker et al., 2022), chloranthranilprole, a new anthranilic diamine insecticide antagonist of ryanodine receptors (Meng et al., 2022) and trifloxystrobin, a strobilurin fungicide with non-target effects involving the stop of respiratory activity in mitochondria (Wang et al., 2021) were targeted due to their

high specific toxicity against benthic macroinvertebrates. Fluopyram and chloranthraniliprole, with high K_{ow} (n-octanol-water partition coefficient), are persistent in water/sediment systems while trifloxystrobin is not due to hydrolysis into trifloxystrobin acid (Feng et al., 2020).

Ultra-pure water (UPW) for extraction and LC-MS analysis was generated using a Millipore system, while methanol (MeOH), ethyl acetate, and HPLC-grade acetonitrile (ACN) were purchased from Carlo Erba Reagents S.A.S. (Val de Reuil, France).

2.2. Experimental design

The design of the column experiment aimed to replicate the collective impact derived from sorption and (bio)degradation on the destiny of specific OMPs within a lateral hyporheic zone (referred to here as 'horizontal zone') experiencing dry conditions. Although the term suggests a horizontal flow direction, this was simulated using a vertical column setup with upward water flow to effectively mimic natural horizontal flow conditions while maintaining practical control over the experiment. In other studies, standardized lab column experiments have been conducted to investigate the transport/sorption and degradation of targeted organic micropollutants (Banzhaf and Hebig, 2016). This yields results that are fully comparable and transferable between different column experiments, avoiding replicates. More specifically, a standardized setup means a column in an upright position with an upward water flow direction. This was accomplished through two column experiments conducted under saturated flow conditions at ambient temperature (approximately 18 °C for both air and water). Due to the complexity of these studies, the number of the columns was limited to two: one for degradation kinetics studies and one for TPs identification. Long glass columns (20 cm) with large diameter (10 cm) and a volume of 6.28 L were used to avoid preferential flow between the inner column surface and the sediment and to allow for the establishment of redox zoning. To prevent OMP photodegradation processes and algae growth, the columns were enveloped with aluminum foil. Peristatic pumps were used to provide uniform flow at modest flow rate of 1 mL min^{-1} (on average), aligning with estimated surface flow velocities at the field site where sediment and water were sourced. Under these conditions, an average hydraulic residence time (HRT) of 42 h was determined. This method was chosen to prevent issues arising from gas accumulation within the column and did not affect the accuracy of the method, with vertical flow assumed to be similar to the actual horizontal river flow. Surface sediment (1–15 cm deep) and water from the Vidourle River, which is an intermittent Mediterranean river located in the Northern part of Montpellier (France), were collected at the same location downstream of the discharge of a municipal wastewater treatment plant (~0.2 km) using either a core sampler or 20 L amber PET containers. The collected sediment was a sandy sediment with a small silt fraction (4%). It was low in organic matter content (fraction of organic carbon, f_{oc} = 0.2%) and was stored at 4 °C before use.

Before introducing the sediment into the column, it underwent wet sieving to eliminate grain sizes exceeding 2 mm, facilitating the proper packing of the column. The sediment, with an average density of 1.4 g cm^{-3} was subsequently added to the column in small increments and compacted after each addition. This process aimed to eliminate potential preferential flow pathways, ensuring a uniform distribution. The river sediment was installed wet in small layers (1–2 cm) that were individually compacted with a stamp so that the resulting effective porosity (0.4) was similar of that of the natural river sediment. Prior to the actual experiments, the column underwent flushing with non-spiked influent river water to stabilize the system until consistent values for the physical-chemical parameters of the effluent water were achieved. Details regarding the quality of the inflowing river water are presented in Table 1. This adaptation phase lasted over one month, minimizing the impact of potential temporal fluctuation in water composition, ensuring the establishment of equilibrium conditions at the experiment's outset and promoting the growth of biofilms in the columns, as outlined by Banzhaf et al. (2012). Previous lab column experiments under water saturated conditions only involving one column have been already published to investigate the fate of organic micropollutants (Zeeshan et al., 2023; Banzhaf et al., 2012).

The column experiments consisted of two steps. In the first step, columns were operated under saturated flow conditions during two weeks. Water was then removed from columns by gravity to simulate a desiccation period of 5 weeks. Then, the water flow was reinitiated for two additional weeks. The two columns were operating in different conditions in order to obtain reliable results for both kinetic studies related to pharmaceuticals and pesticides degradation, and TPs formation. The first column (referred from now on as kinetic column) was fed with a wastewater dominated river water spiked with targeted OMP at 1 μg/L each for kinetic studies. The concentrations of targeted pharmaceuticals and pesticides including venlafaxine TPs (i.e., venlafaxine-N-oxide, N-desmethylvenlafaxine and O-desmethylvenlafaxine) in inflow river water were below 50 ng/L and did not have a significant impact on the spiking level (results not shown). This column was operated in a continuous flow mode without water recirculation to simulate the real river flow. In this way, water was entering to the column from one storage tank, that was refilled with fresh river water to keep the column filled. Inflow river water was renewed every 3 days so that chemicals remain stable in storage tanks. The water exiting the column was collected in an outlet tank, which was emptied on a daily basis. Spiking was implemented to avoid the inconsistent and too low occurrence levels of OMP in river waters over a long period.

The second column (referred from now on as TP column) was fed with the same river water but spiked with targeted OMP at 1 mg/L for TPs identification except for chloranthraniliprole and trifloxystrobin which were spiked at 0.5 and 0.8 mg/L because of their respective water solubility level (see Table S1). This column was operated in a closed loop mode which was considered to be the best choice for TPs detection, thus avoiding the loss of TPs in the case of a continuous flow. Effluent was collected in one tank from which water entered the column system and recirculated back to the same tank from the column outlet, keeping the column full with the same water and thus, preventing any water or TPs from being lost. In kinetic studies, the reduction of the target compounds was assessed by examining the concentrations entering and exiting the column (C/C_0) over a 14-days period. Water samples (250 mL) were collected at regular daily intervals in glass bottles starting at day 3 (corresponding to 48 h). Sediments from three different sections of the column were also collected from the column after the experiment to

Table 1
Major column influent and effluent water characteristics before (Inf. and Eff.1) and after the five-weeks sediment desiccation period (Eff.2) as well as DNA amount in water and sediment before and after the desiccation period (Sed. 1 and Sed.2, content average at three levels along the column). Measures were done in duplicate for both kinetic and TP columns. Means including values from both columns are depicted here.

Parameter	Inf.	Eff. 1	Eff. 2	Sed. 1	Sed. 2
pH	7.6 ± 0.1	7.6 ± 0.1	7.7 ± 0.1	–	–
Electrical conductivity (μS/cm)	780 ± 16	790 ± 17	780 ± 16	–	–
NO_3^- (mg/L)	20.9 ± 0.1	20.9 ± 0.1	2.4 ± 0.1	–	–
DOC (mg/L)	7.3 ± 1.1	5.9 ± 0.6	6.4 ± 0.4	–	–
DNA amount (μg/L or μg/g)	2.8 ± 0.2	1.4 ± 0.1	4.2 ± 0.5	1.7 ± 0.6	1.1 ± 0.1

evaluate possible sorption of the compounds of interest.

2.3. Water and sediment samples extraction and analysis

Water samples were filtered with 0.45 μm syringe filters made of nylon. After that, the 1 mg/L spiked samples were directly injected in LC-HRMS for TPs indentification. Solid phase extraction (SPE) was performed for water samples spiked with 1 μg/L compounds mix for kinetic studies using Oasis HLB (200 mg/6 cc) cartridges. The cartridges were conditioned with 6 mL H_2O and 6 mL MeOH and eluted with 6 mL MeOH. After being concentrated under stream of nitrogen and reconstituted in 250 μL 10% MeOH, final extracts were analyzed by suspect and non-target LC-HRMS workflows following the method developed by Tadić et al. (2022).

Sediment samples were analyzed following a methodology previously developed by Banzhaf et al. (2012) with slight modifications. Sediments were collected at different column sections (0–5 cm, 5–10 cm and 10–15 cm) to confirm or exclude the presence of the selected OMP and thus, possible sorption mechanisms. A total of 5 g (dw) of homogenized sample was spiked with 10 μL of the IS mix (200 ng of each IS) and suspended with 30 mL MeOH/ethyl acetate (15:10, v/v) mixture. The samples were extracted by ultrasound at 25 °C for 30 min, and left at 4 °C for 12 h before centrifugation (10 min at g-force of 1699×*g*). Finally, supernatants were evaporated under a gentle stream of nitrogen at 40 °C, mixed with 1 mL MeOH and transferred to a 2 mL vial for their analysis. Recovery values were in the 60–80% range according to the compound and limits of detection (LODs) were below 10 ng/g.

Details about the instrumental parameters for chromatographic analysis and MS detection are reported in SM.

For TPs identification, we combined a suspect and non-target screening for the better elucidation of known and possibly first-identified TPs. We first performed a literature search of the most common and already identified environmental TPs to be able to establish a list of suspect metabolites for their subsequent screening in (bio) degradation samples (see Table S2). Using the suspect list, the molecular ions $[M + H]^+$ were isolated from the chromatograms obtained through (+)ESI-HRMS, with an isolation width of 5 ppm. Tentative identifications were then corroborated by considering their relative retention times (RT) and, when accessible in the literature, their MS2 spectra. MS data for detected TPs are reported in Table S3. Compound Discoverer 3.3 (Thermo Fisher Scientific, CA, USA) was used for non-target TPs identification, defining a workflow following specific criteria such as: selection of spectra, blank subtraction, peak picking, RT alignment, assignment of isotope and adduct peaks of the same compound into one group, molecular formula assignment, selection of relevant peaks for identification and candidate comparison with the mzCloud software-linked MS2 library. Identification parameters were at least 2 fragments, mass tolerance of 5 ppm, intensity >1000, while 80% for the isotopic match was a threshold for confirmation. DDA-MS2 run was set with an inclusion list of the masses selected after prioritization made using Compound Discoverer 3.3 and the compiled suspect list from literature (see suspect list in Table S2). DDA was conducted with a resolution of 17,500 FWHM for fragmentation products, utilizing two absolute collision energies (20 eV and 40 eV), an isolation window of 1 *m/z*, AGC set at 5×10^4, a maximum ion injection time of 150 ms, and a scan range of 50–1000 *m/z*. The resulting TPs spectra were cross-referenced against online databases such as mzCloud, MassBank, and MoNA for final confirmation whenever available, achieving identification level 2 based on the acquired MS2 spectra (Schymanski et al., 2014). In cases where such confirmation was not available, identification reached level 3.

2.4. DNA extraction

DNA extraction was performed with the DNeasy® PowerWater® kit (Qiagen) for water samples and the FastDNA™ SPIN Kit for Soil (MP Biomedical) for sediment samples. The kits were used according to the protocol provided by the manufacturer. DNA purity and concentrations were estimated by spectrophotometry (Infinite NanoQuant M200, Tecan, Austria). DNA samples were stored at −20 °C before sequencing.

2.5. Illumina sequencing

The V4 and V5 variable regions of the 16S rDNA gene were amplified utilizing the primers 515 U (5′ -GTGYCAGCMGCCGCGGTA −3′) and 928 U (5′ - CCCCGYCAATTCMTTTRAGT −3′) as detailed by Venkiteshwaran et al. (2016). Adapters were introduced during the second amplification step for the purpose of sample multiplexing. The resultant products underwent purification and were then loaded into the Illumina MiSeq cartridge for sequencing, employing paired-end reads with a length of 300 bp (2X300 sequencing) following the manufacturer's recommendations for v3 chemistry. The sequencing and data library preparation were conducted by the Genotoul Lifescience Network Genome and Transcriptome Core Facility in Toulouse, France (get.genotoul.fr). Mothur (version 1.48.0) (Schloss et al., 2009) was utilized for read pairing, sequence filtering, and clustering. UCHIME was employed to eliminate chimeras, and sequences occurring fewer than three times across the entire dataset were excluded. Alignment of sequences was carried out using the SILVA database SSURef NR99 version 132 (Schloss et al., 2009). Sequences sharing 97% similarity were grouped into operational taxonomic units (OTUs).

2.6. Real time quantitative PCR (qPCR)

Amplification reactions were performed in reaction mixtures (12 μL) containing 6 μL of Sybr Super Mix (Biorad) and primers at concentrations indicated in supplementary material (Table S6). Total bacterial quantification was performed by qPCR targeting the V3 region from 16S rDNA. Genes related to nitrogen cycle (nitrate reductase, *narG* and bacterial ammonia mono-oxygenase: *amoA*-B) were quantified. qPCR programs and primer's list are available in supplementary methods and Table S6.

For 16S rDNA, *narG* and *amoA*-B the qPCR programs consisted in initial denaturing at 95 °C (2 min), followed by 40 cycles at 95° (15 s or 10s for 16S rDNA) for denaturation and Ta (Table S6) (60 s or 20s for 16S rDNA) for annealing and amplification. The fluorescence data was acquired at the annealing temperature or at 72 °C for acrB and nirS, and the final melting curve was constructed with temperature ramping up from 72 °C to 95 °C.

3. Results and discussion

3.1. Fate and transport of targeted compounds in column experiments (kinetic studies)

Some important parameters including nitrate and DOM of river water are reported in Table 1. The experiment did not consider a limitation of nitrogen in the column, as nitrate ions were consistently detectable at the column outlet throughout the entire duration of the experiment. During the first biodegradation phase (before the desiccation period), the nitrate concentration at the column outlet remained similar to that at the inlet (20.9 ± 0.1 mg/L). However, after the desiccation period, the nitrate concentration at the outlet decreased to 2.4 ± 0.1 mg/L, meaning that the drying period induced or favored denitrification process within the column. Several studies have suggested that the desiccation of sediments could stimulate the rates of nitrogen transformation such as nitrogen mineralization, nitrification and denitrification, which could happen in this study (Baldwin and Mitchell, 2000; Gómez et al., 2012; Pinto et al., 2021). There was no observable iron and manganese reduction resulting in non-measurable concentrations of Mn^{2+} nor Fe^{2+} at the outlet of the column. A gradient of redox conditions was therefore established with an oxic zone

at the inlet which was then followed by nitrate reducing conditions, following the desiccation period. DOC concentrations slightly dropped from 7.3 ± 1.1 mg/L (inlet) to 5.9 ± 0.9 mg/L (outlet) before the desiccation period and to 6.4 ± 0.4 after the desiccation period. A significant portion of the observed reduction in oxygen and nitrate can be attributed to the oxidation of organic carbon bound to the sediment, as previously noted (Baldwin and Mitchell, 2000). The presence of a small amount of biodegradable dissolved organic carbon (DOC) at a few mg/L likely supported microbial activity and contributed to the probable degradation of OMP (Mueller et al., 2021).

The breakthrough curves of the OMP measured at the column outflow are graphed in Fig. 1 before and after the desiccation period. The measured concentrations were modeled using pseudo-first-order dissipation kinetics to obtain removal rates (k_{app}) and related half-lives (DT_{50}) values. The related k_{app} and DT_{50} are reported in Table 2. Total DNA concentrations in sediment were used to estimate active biomass for DT_{50} normalization because higher biomass levels can lead to higher biodegradation. However, no significant differences in DNA concentrations were found before and after the desiccation period (see Table 1). The compound breakthrough was most likely due to either sediment sorption and/or (bio)degradation processes, as one of the two mechanisms is expected to be the primary cause. To assess the significance of sorption, the sediment material was extracted from the column upon completion of the experiment. Subsequently, samples from three segments of the column were collected and analyzed for the targeted compounds. None of the compounds were detected at concentration levels above LODs (i.e., 10 ng/g). Consequently, sorption did not significantly contribute to the compounds dissipation in spite of very contrasting Log P and Koc values (Table S1), and observed dissipation was mainly attributed to biodegradation. However, this outcome was anticipated, considering the sediment's deficient sorptive capacity due to its low carbon content (<0.2%) and a limited proportion of fine minerals. Cationic exchange at anionic surfaces within the sediment was anticipated for compounds with cationic properties, such as antidepressants. Nevertheless, an examination of the cation exchange capacity confirmed that the collected sediments exhibited poor sorptive properties for cations, with a median cation exchange capacity of 0.5 and a maximum of 2.6 cmol/kg. This was likely attributed to the low fraction of fine mineral material, with particles smaller than 0.063 mm constituting less than 0.1%.

For neutral pesticides (especially those with high log P) sorption was expected in particular due to the presence of biofilms. However, sorption was most likely minimized in continuous flow mode. At the first sampling time (t = 3 days), the outlet concentrations did not reach the influent concentrations except for chloranthraniliprole before sediment desiccation, and for fluopyram and paroxetine after the desiccation period. This result meant that biodegradation started during HRT (42 h) being faster for amisulpride, trifloxystrobin and venlafaxine. At day 3, the outlet concentrations of amisulpride, trifloxistrobin and venlafaxine after the desiccation period were lower than before. Amisulpride and venlafaxine reached half of the initial spiking concentration of 1 μg/L, with concentrations of 0.47 μg/L and 0.48 μg/L at day 3, respectively. Trifloxistrobin also had a faster decrease in concentrations, passing from a concentration of 0.89 μg/L before desiccation to 0.71 μg/L after desiccation at day 3. After day 3, the contaminants underwent a decrease in concentrations to different extent due to differences in biodegradation levels. Amisulpride was the compound that underwent faster decrease, reaching a complete degradation at day 10. Similarly, venlafaxine degraded rapidly, with its concentrations halving within 3 days (0.48 μg/L), dropping to 0.25 μg/L after 7 days, 0.12 μg/L after 12 days, and disappearing entirely by day 14. On the other hand, chloranthraniliprole and paroxetine presented slower degradation rates, with both concentrations decreasing from 0.98 μg/L at day 3 to 0.8 μg/L at day 14 after desiccation.

Table 2
Removal rates (kapp) and related normalized half lives (DT50) of targeted compounds before (1) and after (2) the desiccation period of sediment.

Compound	$k_{app}(d^{-1})$ (1)	DT_{50} (d) (1)	$k_{app}(d^{-1})$ (2)	DT_{50} (d) (2)
Amisulpride	0.17	4.08	0.201	3.44
Fluopyram	0.063	11.0	0.11	6.3
Venlafaxine	0.039	17.77	0.193	3.59
Chloranthranilprole	0.0191	36.28	0.0167	41.5
Paroxetine	0.0165	42.0	0.0184	37.66
Trifloxystrobin	0.0284	24.4	0.0661	10.48

Potential abiotic transformation reactions were assumed irrelevant. Experiments were performed in the dark and phototransformations could be therefore excluded. Other abiotic redox reactions could not be ruled out at first due the presence of iron and manganese oxides in the collected sediment. However, since sorption processes were found to be insignificant for the targeted compounds, these reactions were excluded. Finally, it is known that corrinoids are produced by typical sediment microorganisms (e.g., methanogenic archaea) and prevalent in sediment and water under reducing conditions, catalyzing abiotic dehalogenation reactions (El-Athman et al., 2019). However, these reactions required stronger reducing conditions than the ones corresponding to denitrification (i.e., anoxic conditions) to operate and could therefore be discarded.

A significant reduction in concentration was noted for the majority of

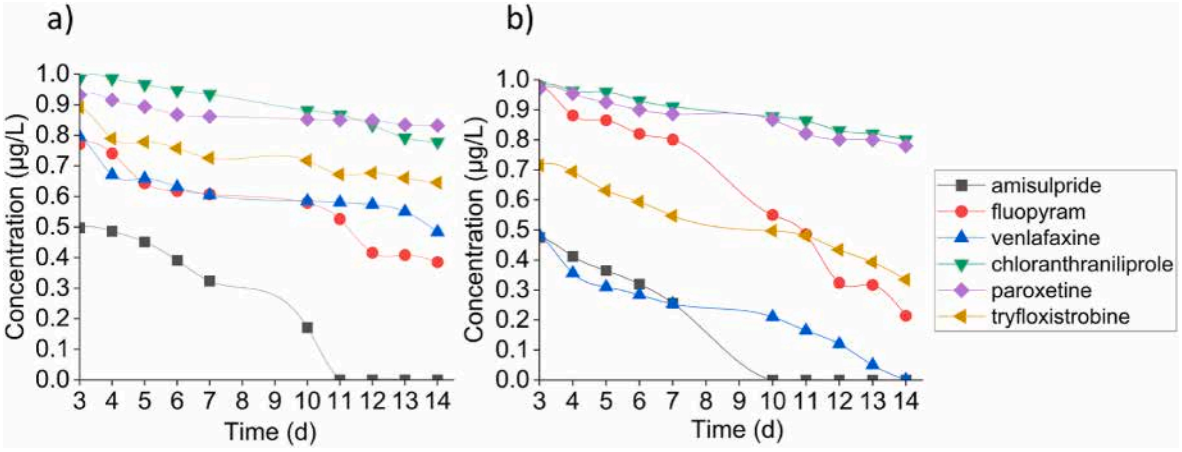

Fig. 1. Time series of concentrations of investigated compounds revealing degradation kinetics during infiltration of river water spiked at 1 μg/L (each compound) into a column filled with river sediment starting from day 3 of the experiment measured at the outflow of the column before (a) and after (b) the desiccation period. Day 3 (48 h) was used as start data because the water needed 42 h to flow through the column (hydraulic residence time).

compounds, affirming the impact of HZ infiltration in enhancing biodegradation. DT_{50s} ranged from 4 days (amisulpride) to 42 days (paroxetine). The most persistent compounds were chloranthraniliprole and paroxetine while the most labile compound was amisulpride. Fluopyram, venlafaxine and fluoxystrobin showed intermediate behaviors. These results are consistent with previously reported ones in water-sediment systems (see Table S1). Two exceptions were fluopyram and trifloxystrobin. Trifloxystrobin was reported to undergo fast hydrolysis into fluoxystrobin acid with a $DT_{50} = 2.4$ days (see Table S1), while in this work its dissipation was slower ($DT_{50} = 24$ days). In contrast, fluopyram was considered persistent in water/sediment ($DT_{50} > 1000$ days) system (Rathod et al., 2022), while in this work it dissipated much faster ($DT_{50} = 11$ days).

Results obtained after the desiccation period were significantly different for venlafaxine, trifloxystrobin and fluopypam while similar for paroxetine, amisulpride and chloranthraniliprole. Persistent compounds and readily biodegrable compounds were therefore not impacted by the dryness period, while moderately biodegradable compounds showed increased biodegradation rates with two-folds decrease in DT_{50} for fluopyram and trifloxystrobin and even five-fold decrease for venlafaxine. The prior exposure to chemicals from wastewater treatment plant (WWTP) discharge or agricultural water runoff likely heightened bacterial biodegradation. The rapid dissipation suggests the widespread presence of bacteria with the capability to degrade these compounds.

3.2. Identification of transformation products and elucidation of transformation pathways

The level of confidence for the identified TPs was assigned on the basis of the Schymanski et al. (2014) system. Four TPs were confirmed by the availability of analytical standards (confidence level 1). Ten TPs were determined via a suspect screening workflow (confidence level 2) and 6 TPs were tentatively identified by a non-target screening approach (confidence level 3). On the basis of TPs identification (see MS data in Table S3), the tentative degradation fates of targeted pesticides and pharmaceuticals are presented in Fig. 2.

Chloranthraniliprole: The non-detection of this TP resulting from intramolecular cyclisation of chloranthraniliprole with concomitant water losses was the least expected, since this TP was previously found to be the main TP in soil (Redman et al., 2019). In contrast, TP470 originating from the amide hydrolysis into carboxylic acid was identified, while this latter transformation was never observed in soil. TP439 was also detected by the non-target screening approach at a RT higher than the parent compound accounting for more hydrophobic properties. A $C_{17}H_{13}BrCl_2N_4O$ theoretical elemental composition was assigned to this TP with a high confidence level (mass error below 5 ppm). TP439 might result from further transformation of TP470 through decarboxylation of the derivative of benzoïc acid and through methylation of benzene by a methyl transferase. The alkylation of benzene to toluene has been found an interesting hypothesis for anaerobic benzene degradation in microbial systems (Ghattas et al., 2017) and occurred for instance during the HZ biodegradation of benzotriazole (Posselt et al., 2020). Double bond equivalent (DBE) data, extracted by MS data for detected TPs in our study, was consistent with the proposed structure with one-unit decrease of DBE (11.5) in comparison to chloranthraniliprole (12.5) due to carbonyl moiety losses.

Fluopyram: fluopyram was degraded following three competitive routes. An oxidative route involved one or two hydroxylation reactions (TP413 and TP429, respectively). Hydroxylation at the functional group C7 was specifically discarded because this transformation has usually been followed by microbial cleavage of nitrogen-carbon bond as previously observed in plant and soil (Wei et al., 2016) and known TPs resulting from this cleavage were not detected. The exact location of hydroxyl groups was unknown and a level of confidence of 3 was therefore assigned, even though a dihydroxylation reaction at C7 and C8 was already reported under photochemistry (Mekonnen et al., 2018). A new reductive transformation route involved a dechlorination reaction in combination to dehydrogenation reaction (i.e., fluopyram-olefine) leading to TP360. Finally, a hydroxy-substition route already identified under direct photolysis led to TP379 (Dong et Hu, 2016).

Trifloxystrobin: The present study confirmed that hydrolysis of the ester moiety is the major environmental transformation pathway of

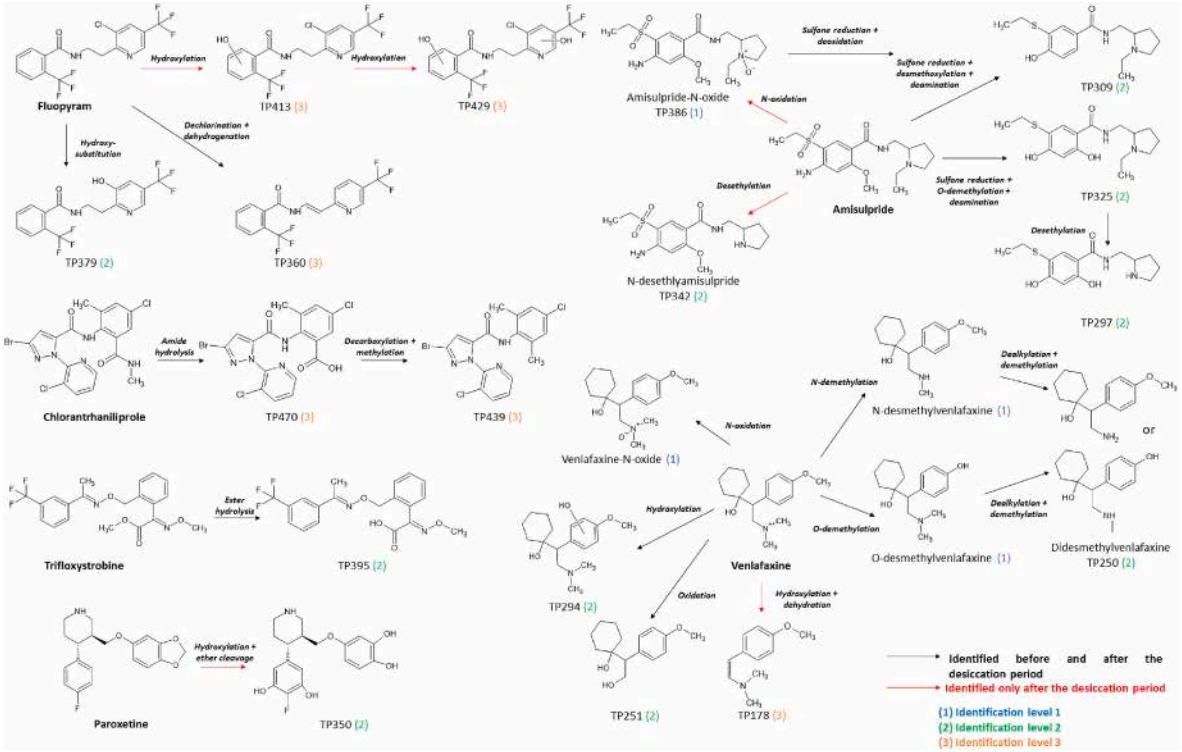

Fig. 2. Tentative transformation pathways of targeted compounds. Identification levels of confidence are based on Schymanski system (Schymanski et al., 2014).

trifloxystrobin with trifloxystrobin acid (TP395) generation (Abdourahime et al., 2019; Jiang et al., 2022).

Paroxetine: The ether bond exhibits chemical and biological inertness. However, aromatic methoxy groups are known to be cleaved under anaerobic conditions leading to the corresponding phenol (Ghattas et al., 2017). Ether cleavage was most likely preceeded by hydroxylation reactions in the oxic zonation of the column leading to TP350, as the unique TP detected for paroxetine. The most probable location of the hydroxy groups is in *ortho* positions of the F substituent as theses positions are the most nucleophilic ones. TP350 has already been identified under photochemistry (Gornik et al., 2021).

Amisulpride: The present study confirmed the relevance of the formation of amisulpride-N-oxide (TP386) and N-desethylamisulpride (TP342) as observed in water/sediment systems under aerobic conditions (Manasfi et al., 2022). Interestingly, reduction processes were observed including reduction of sulfone into sulphide (TP309, TP297 and TP325) similarly to the reduction of fipronil into fipronil sulphide under anoxic conditions (Tomazini et al., 2021). Similarly to sulfamethoxazole under denitrifying conditions (Brienza et al., 2017), amisulpride might undergo nitrosative deamination through the formation of a diazonium salt which was unstable and could be hydrolyzed into hydroxy-amisulpride (TP309, TP297 and TP325) followed by O-desmethylation (TP325 and TP297) or desmethoxylation (TP309) as previously observed under photocatalysis (Antonopoulou et al., 2023). The chemical structures of TP317, TP365 and TP425 could not be elucidated.

Venlafaxine: Venlafaxine-N-oxide as well as N- and O-desmethylvenlafaxine already occurred in inflow river water making their source assignment difficult. In contrast, hydroxylation (TP294) reaction was confirmed inside the column (TP 294) because hydroxylvenlafaxine eluates before venlafaxine, while venlafaxine-N-oxide eluates after venlafaxine under C-18 reverse phase chromatographic conditions (Manasfi et al., 2022). N-desmethylvenlafaxine and O-desmethylvenlafaxine underwent further O- or N-dealkylation reactions leading to two didesmethylvenlaxine isomers (TP250). As previously described by Barbieri and Chiron (2023), TP251 can arise from a one-electron oxidation reaction at the C located in α position of the N atom. This reaction occurred due to the stabilization of the resulting radical through resonance, allowing for further neutralization to yield a primary alcohol (TP251). The structure of TP178 could not be conclusively determined. However, one hypothesis might be a hydroxylation reaction at the benzylic position followed by dehydration reaction.

As a whole, oxidation and reduction processes successively occurred following the redox zonation in the column allowing for multiple transformation routes for most of the targeted compounds. TPs identification revealed that transformation reactions which are common for oxic conditions such as hydroxylation and N-dealkylation were associated with reductive dehalogenation, sulfone reduction or O-demethylation reactions which are relevant for denitrifying conditions. A more accurate oxygen measurement at the outlet of the column would have been necessary to refine its role. This study demonstrated the strong dependency of amisulpride, fluopyram and venlafaxine transformation specifically on nitrate reducing redox conditions similarly to sulfamethoxazole (Banzhaf et al., 2012). Anaerobic conditions are capable of enhancing the transformation of contaminants that use to persist in aerobic conditions (Völker et al., 2017). The varying redox conditions (redox zonation) as well as the related variation in microbial communities along the column flowpath rendered therefore the simulated HZ an efficient (bio)reactor for compound removal. Additional transformation routes for fluopyram and venlafaxine after the desiccation period (red arrow in Fig. 2) might account for their higher (bio)degradation kinetic rates. Oxidation reactions (e.g., hydroxylation, N-oxidation) mostly accounted for these additional transformation routes. However, this did not hold true for amisulpride and paroxetine for which additional transformation routes were also detected, while k_{app} remained similar, without a clear explanation for these experimental results. Chloranthraniliprole and trifloxystrobin TPs were shared by both experimental conditions logically leading to similar kinetics, confirming that hydrolysis reactions are less sensitive to variation in environmental conditions. Temporal dynamics of common TPs (on the basis of peak intensity) were also determined (see Fig. S1) to investigate the potential exacerbation of specific and common transformation routes before and after the desiccation period. Only the formation of TP325 of amisulpride (reductive route) clearly underwent a sharp increase in peak intensity after the desiccation period, while the other TPs peaks mostly remained unchanged. Variations in degradation kinetic rates was therefore more related to the appearance of new transformation routes than to the alteration of the relative significance of existing transformation routes. Although the elevated concentrations used in this study may not accurately reflect the environmental concentrations typically encountered in natural systems, they serve as an effective tool for identifying a wide range of potential TPs. We acknowledge that such high concentrations could potentially lead to artefacts—unrealistic processes that would not occur under more typical environmental conditions. Although artefacts could not be completely ruled out, the identification of TPs in lab-scale experiments provides a useful starting point for further investigation of their formation under more realistic environmental conditions.

3.3. Evolution of microbial communities

Regarding the kinetic column experiment, the richness (Observed and Chao1) and diversity (Shannon) indices remained at the same order of magnitude between the inlet and outlet of the column (see Table S4). Consequently, environmental OMP concentrations did not disturb the richness and diversity of the water compartment. A different trend was observed for the sediment compartment where the desiccation period had a negative impact on the bacterial richness and diversity (see Table S5). As expected, for the TP column experiment, higher OMP concentrations resulted in a drop of the diversity indices (see Tables S4 and S5).

Structure of bacterial community was also impacted by desiccation period. Fig. 4 shows the evolution of the main phyla and genera in water for both the kinetic and TP columns experiments. It could be seen that after the first biodegradation phase, the proportion of Proteobacteria decreased from 53% to 50% in kinetic column and to 39% in TP column. Firmicutes, and Actinobacteria behaved similarly in kinetic column, whereas an increase of the relative abundance was observed for Acidobacteria and Hydrogenedentes (from 1% for both phyla to 4% and 2% respectively). Planctomycetes increased also in both kinetic and TP columns from 3% to 11% and to 12% respectively, while Verrucomicrobia only increased in TP column (from 3% to 20%). Verrucomicrobia and Planctomycetes have a high tolerance for non-steroidal anti-inflammatory drugs and some other pharmaceuticals, which could explain their high abundance in TP column experiment (Farkas et al., 2023). Furthermore, they were both initially present in river water at T0 and identified as indicator taxa of wastewater treatment plant effluent dominated sites, suggesting a possible contamination of river water (Romero et al., 2019). After the desiccation period, the relative abundance of Proteobacteria continued to decline (Fig. 4). This decrease was primarly associated with a reduction of the relative abundance of some genera from the Methylophilaceae family and some *Legionella* species, likely resulting in wastewater discharge upstream, which contaminated the river (Romero et al., 2019; Marti and Balcazar, 2014). In this context, the sediment column may act as a buffer or filter, reducing their abundance. Conversely, other microbial groups emerged. In the kinetic column, an increase in nitrifying bacteria from the *Nitrospira* genus was observed (Fig. 4). *Nitrospira*, able to perform complete nitrification, also demonstrates resilience to various organic contaminants (Palomo et al., 2018) and is particularly promising for the treatment of contaminated sediments due to its potential bio-augmentation effect (Veloso et al., 2023). In the TP column experiment, a significant increase in the

proportion of Bacteroidetes was observed, especially in the genera *Candidatus Aquisteris* and *Dyadobacter* (Fig. 3). *Candidatus Aquisteris,* belonging to the Saprospiraceae family, is known as a denitrifying bacterium and degrader of complex organic compounds (De Carluccio et al., 2023; Sun et al., 2012). *Dyadobacter* is also an aromatic pollutant degrader, involved in PAH hydroxylation (Willumsen et al., 2005), nitrifying processes and used for bioremediation (Bucci et al., 2021; Yadav et al., 2021). Thus, it appears that the desiccation period favored the growth of nitrifying and denitrifying bacteria, as already observed in previous studies (Gómez et al., 2012; Pinto et al., 2021). These nitrifying/denitrifying bacteria could therefore be linked to the emergence of new OMP transformation pathways identified during the second phase of biodegradation, including the presence of N-oxide derivatives of amisulpride and fluopyram for instance.

In sediments, the main genera observed at the beginning persisted throughout the experiment, which might be explained by the low OMP sorption in this compartment, thus causing little disturbance to bacterial communities (Fig. S2). At T0, sediment samples were dominated by Proteobacteria (42%), Firmicutes (42%) and Actinobacteria (10%). Over the experiment, the proportion of Actinobacteria was reduced (<2%), while the main genera present among Proteobacteria (largely represented by *Ralstonia*) and Firmicutes (Bacillaceae including the genera *Bacillus*, *Brevibacillus*, *Geobacillus*, *Hydrogenispora* and certain genera of the Thermoactinomycetaceae family) persisted. In other studies, desiccation period led to the decrease of Proteobacteria and Bacteroidetes and the increase of Alphaproteobacteria and Actinobacteria (Romero et al., 2019). The opposite effect is observed here. It is therefore possible that the changes brought by periods of desiccation are ecosystem-dependent and driven by pre-established endogenous microbial communities.

Ralstonia and members of the Bacillaceae family are known to be both pollutant degraders that can be found in sediments (Arora, 2020; Coll et al., 2020; Ferreira et al., 2016; Ryan et al., 2007). Their relative abundance was modulated according to the different stages, and although the microbial composition before and after the drying period was similar (Fig. S2), the restart of the water flow resulted in a sharp increase in the proportion of *Ralstonia* in both columns, accounting for 62 % and 68% of the total diversity at the end of the experiment. *Ralstonia*, a denitrifying bacterium, was identified as a marker of fast OMP dissipation, including venlafaxine transformation into O-desmethylvenlafaxine (Coll et al., 2020). The increase of the abundance of this genus could be linked to the increase of degradation rates observed after the desiccation stage.

3.4. Evolution of 16S rDNA gene and nitrogen functional genes narG and amoA-B

The qPCR analyses were achieved on 16S rDNA gene, *narG* gene encoding the membrane-bound nitrate reductase and used as a proxy of denitrification processes and *amoA*-B gene, encoding for the bacterial ammonia monooxygenase and related to nitrification processes (Fig. 4, Tables S7–S8).

16S rDNA results showed that in water, the same copy number was found at T0 and in kinetic column (Fig. 4a). In the TP column, the first phase of flowing water spiked with OMP at 10 mg/L resulted in a drop in the number of 16S rDNA copies (−0.5 log), in concordance with the reduction in diversity and richness potentially due to the bacterial toxicity of some OMPs including fluopyram, chlorantraniliprole and paroxetine (Zhang et al., 2014; Wu et al., 2018; Foletto et al., 2020; Tables S4–S5). However, after the desiccation period, a significant increase was observed (+1.1 log), which can be hypothesised to be linked to the increase in the relative abundance of Bacteroidetes (Fig. 4). In the sediments, the first circulation of water led to a sharp increase in the number of copies of 16S rDNA in the kinetic column (+3.1 log, Fig. 4d). After the desiccation period, a slight decrease was observed (-0.7 log), which then intensified after 17 days (-2.6 logs). Initially, the sharp increase observed could be associated with the supply of nutrients by the river, probably stimulating endogenous bacteria in the sediments. Secondly, the repeated input of potentially toxic compounds present in the river water and the OMPs might have contributed to the observed decrease in bacterial richness and diversity (Table S5). A similar dynamic was observed in TP column to a lesser extent, due to the higher concentration of OMPs. The same type of phenomenon was noted in river sediments downstream of the WWTP discharge (Marti and Balcazar, 2014).

For *amoA*-B gene in water, no significant differences were found between conditions (Fig. 4b). In sediments, although it was below the limit of detection at T0, it was quantified in kinetic column just before and after de desiccation period, suggesting a transfer and/or bacterial interaction between river water and the sediments (Fig. 4e). Thus, in water, even if increase of specific nitrifying bacteria was observed after the desiccation period (*Nitrospira, Dyadobacter*), the global population of ammonium oxidizing bacteria was maintained. The appearance of new oxic transformation pathways of OMPs, such as N-oxidation of hydroxylation type could therefore come from these specific nitrifying bacteria emerging after the desiccation period.

For *narG* gene in water, no difference was observed after the first river water circulating period. However, an increase of 0.6–0.8 log was

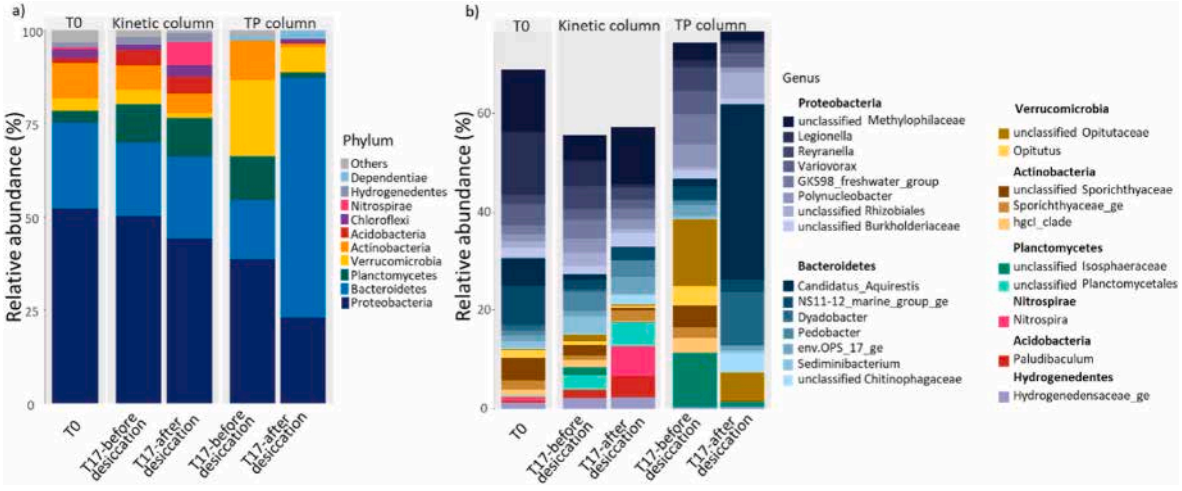

Fig. 3. Bar plot of relative abundance (% reads) of bacterial communities in water from the inlets and outlets of the sediment columns, before and after the desiccation period, (a) at the phylum level and (b) at the genus level (main genera representing more than 1% of the total diversity).

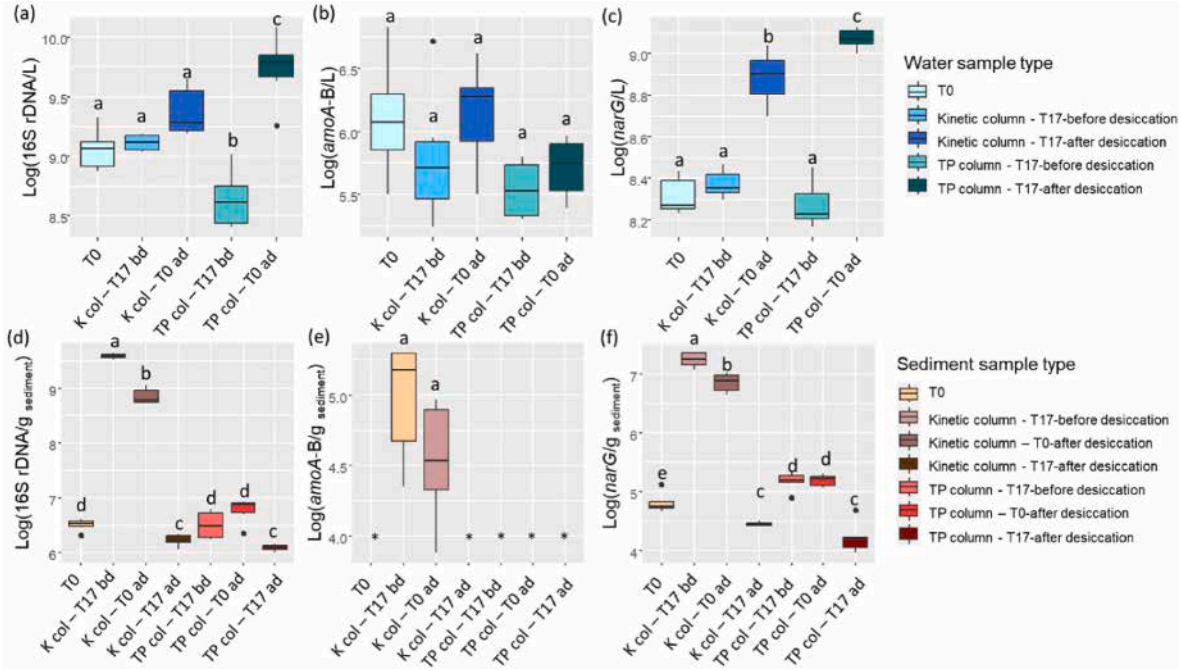

Fig. 4. Dynamic of key genes quantified by qPCR before and after desiccation period in outlet water and sediments. (a) 16S rDNA/L, (b) *narG*/L and (c) *amoA*-B/L in outlet water. (d) 16S rDNA/$g_{sediment}$, (e) *narG*/$g_{sediment}$ and (f) *amoA*-B/$g_{sediment}$ in sediments. bd = before desiccation, ad = after desiccation, T17 = 17 days. * = genes were below the limit of quantification. Letters in the graph indicate significant differences between the conditions (one-way ANOVA, different letters mean that values were significantly different, p value < 0.05). Boxplot were obtained from 6 analytical replicates per condition.

observed after the desiccation period, suggesting an increase of denitrifiers and their activity (Fig. 4c), in agreement with the decrease in nitrate after this period (Table 1). In sediments, the dynamic of *narG* gene followed those of 16S rDNA gene, with a strong increase during the first river water circulating period and then a decrease after the desiccation period (Fig. 4f). The increase in denitrifiers may be due to a decrease in the redox potential in the sediment column when the river water is circulated, as suggested above, and to the relatively high concentration of nitrate in the river water (Table 1). This phenomenon was already observed elsewhere and it was shown that desiccation period induced the increase of denitrifiers (quantified via *narG* gene) compared to wet sediments (Romero et al., 2019). The decrease then could be due to the reduction of nitrate concentration, thus modulating the population of denitrifyers in sediments, probably related to Firmicutes phylum. The opposite effects observed between water and sediments suggest interactions and transfers between these two matrices and the stimulation/modulation of denitrifying bacteria could be at the origin of the acceleration of anoxic transformation pathways such as reductive transformation of OMPs.

However, their activity could also be linked to oxic transformation and most specifically to hydroxylation. In anoxic/denitrifying conditions, some studies have reported enhanced hydroxylation pathways due to syntrophic relationships between microorganisms. In the absence of oxygen, microbial communities can utilize a range of alternative electron acceptors such as nitrate, manganese oxides, iron oxides, sulfate, or CO_2 generated from organic matter degradation. The redox potentials of these electron acceptor systems influence both the energetics and kinetics of reactions, and can also dictate the pathways for degrading organic contaminants. For example, resorcinol was reduced to cyclohexa-1,3-dione using reduced benzyl viologen, which has a redox potential of −790 mV—difficult to achieve under anoxic conditions (typically between 200 and -220 mV). However, it was hydroxylated by nitrate-reducing bacteria at a higher redox potential of −100 mV (Schink, 2006). Thus, in our case, the shift of the microbial community towards denitrifiers following the desiccation period may contribute to the enhanced hydroxylation pathways observed here.

4. Conclusions

The lab-scale experiments using columns provided insight into our understanding of the effect of water flow intermittency on OMP biodegradation capacity of the hyporheic zone. Flow intermittency promoted the short-term biodegradation of compounds recognized for their biodegradability, including fluopyram, trifloxystrobin, and venlafaxine. Flow intermittency also increased bacteria capable of degrading these compounds, including nitrifying and denitrifying bacteria. Persistent and easily biodegradable compounds in batch water/sediment tests such as paroxetine, chloranthraniliprole and amisulpride were much less impacted by a desiccation period. Identification of TPs revealed that a combination of oxidative and reductive transformation routes due to a redox zonation inside columns made these latter efficient (bio)reactors for OMP removal. This work contributed to a better knowledge of OMP transformations under anaerobic conditions which are usually less documented than the ones occurring in aerobic conditions. The intermittent stream flow regime can modulate the HZ biodegradation capacity both quantitatively and qualitatively with the formation of different TPs. Some TPs have been reported in this study for the first time, confirming the crucial role of bacteria in the emergence of new degradation pathways. Column experiments allow for capturing the essence of the processes under controlled conditions and at a reasonable cost (in comparison to extensive field experiments) by identifying transformation pathways which are less dependent on initial concentrations than kinetics. OMP attenuation rates transferable to real-world need further research and may include the use of flume experiments to investigate the interactions between controlling factors.

CRediT authorship contribution statement

Maria Vittoria Barbieri: Writing – review & editing, Writing – original draft, Methodology, Investigation, Formal analysis, Data curation, Conceptualization. **Oriane Della-Negra:** Writing – review & editing, Writing – original draft, Data curation. **Dominique Patureau:** Writing – review & editing, Visualization, Supervision, Funding

acquisition. **Serge Chiron:** Writing – review & editing, Supervision, Methodology, Funding acquisition, Conceptualization.

Declaration of competing interest

The authors declare that they have no known competing financial interests or personal relationships that could have appeared to influence the work reported in this paper.

Acknowledgements

This study was funded by the EU PRIMA program as part of the research project INWAT – Quality and management of intermittent river and groundwater in Mediterranean basins (Grant No. 201980E121).

Appendix A. Supplementary data

Supplementary data to this article can be found online at https://doi.org/10.1016/j.chemosphere.2025.144082.

Data availability

No data was used for the research described in the article.

References

EFSA (European Food Safety Authority), Abdourahime, H., Anastassiadou, M., Brancato, A., Brocca, D., Carrasco Cabrera, L., De Lentdecker, C., Ferreira, L., Greco, L., Jarrah, S., Kardassi, D., Leuschner, R., Lostia, A., Lythgo, C., Medina, P., Miron, I., Molnar, T., Nave, S., Pedersen, R., Raczyk, M., Reich, H., Ruocco, S., Sacchi, A., Santos, M., Stanek, A., Sturma, J., Tarazona, J., Theobald, A., Vagenende, B., Verani, A., Villamar-Bouza, L., 2019. Reasoned opinion on the modification of the existing maximum residue level for trifloxystrobin in broccoli. EFSA J. 17 (1), 5576. https://doi.org/10.2903/j.efsa.2019.5576, 25.

Antonopoulou, M., Papadaki, M., Rapti, I., Konstantinou, I., 2023. Photocatalytic degradation of pharmaceutical amisulpride using g-C_3N_4 catalyst and UV-A irradiation. Catalysis 13 (2), 226. https://doi.org/10.3390/catal13020226.

Arora, P., 2020. Bacilli-mediated degradation of xenobiotic compounds and heavy metals. Front. Bioeng. Biotechnol. 8. https://doi.org/10.3389/fbioe.2020.570307.

Baldwin, D., Mitchell, A., 2000. The effects of drying and re-flooding on the sediment and soil nutrient dynamics of lowland river–floodplain systems: a synthesis. Regul. Rivers Res. Manag. 16, 457–467. https://doi.org/10.1002/1099-1646(200009/10)16:5<457:AID-RRR597>3.0.CO;2-B.

Banzhaf, S., Hebig, K.H., 2016. Use of column experiments to investigate the fate of organic micropollutants – a review. Hydrol. Earth Syst. Sci. 20, 3719–3737. https://doi.org/10.5194/hess-20-3719-2016.

Banzhaf, S., Nödler, K., Licha, T., Krein, T., Scheytt, A., 2012. Redox-sensitivity and mobility of selected pharmaceutical compounds in a low flow column experiment. Sci. Total Environ. 438, 113–131. https://doi.org/10.1016/j.scitotenv.2012.08.041.

Barbieri, M.V., Chiron, S., 2023. Relevance of photocatalytic redox transformations of selected pharmaceuticals in a copper- and iron-rich Mediterranean intermittent river. Chemosphere 339, 139762. https://doi.org/10.1016/j.chemosphere.2023.139762.

Betterle, A., Jaeger, A., Posselt, M., Coll, C., Benskin, J., Schirmer, M., 2021. Hyporheic exchange in recirculating fumes under heterogeneous bacterial and morphological conditions. Environ. Earth Sci. 80, 234. https://doi.org/10.1007/s12665-021-09472-2.

Borreca, A., Vuilleumier, S., Imfeld, G., 2024. Combined effects of micropollutants and their degradation on prokaryotic communities at the sediment–water interface. Sci. Rep. 14, 16840. https://doi.org/10.1038/s41598-024-67308-y.

Brienza, M., Duwig, C., Perez, S., Chiron, S., 2017. 4-nitroso-sulfamethoxazole generation in soil under denitrifying conditions: field observations versus laboratory results. J. Hazard Mater. 334, 185–192. https://doi.org/10.1016/j.jhazmat.2017.04.015.

Bucci, P., Coppotelli, B., Morelli, I., Zaritzky, N., Caravelli, A., 2021. Heterotrophic nitrification-aerobic denitrification performance in a granular sequencing batch reactor supported by next generation sequencing. Int. Biodeterior. Biodegrad. 160, 105210. https://doi.org/10.1016/j.ibiod.2021.105210.

Burke, V., Greskowiak, J., Asmuba, T., Bremermann, R., Taute, T., Massmann, G., 2014. Temperature dependent redox zonation and attenuation of wastewater-derived organic micropollutants in the hyporheic zone. Sci. Total Environ. 482–483, 53–61. https://doi.org/10.1016/j.scitotenv.2014.02.098.

De Carluccio, M., Sabatino, R., Eckert, E.M., Di Cesare, A., Corno, G., Rizzo, L., 2023. Co-treatment of landfill leachate with urban wastewater by chemical, physical and biological processes: fenton oxidation preserves autochthonous bacterial community in the activated sludge process. Chemosphere 313, 137578. https://doi.org/10.1016/j.chemosphere.2022.137578.

Coll, C., Bier, R., Li, Z., Langenheder, S., Gorokhova, E., Sobek, A., 2020. Association between aquatic micropollutant dissipation and river sediment bacterial communities. Environ. Sci. Technol. 54, 14380–14392. https://doi.org/10.1021/acs.est.0c04393.

Cunnigham, V., Constable, D., Hannah, R., 2004. Environmental risk assessment of paroxetine. Environ. Sci. Technol. 38, 3351–3359. https://doi.org/10.1021/es035119x.

Dong, B., Hu, J., 2016. Photodegradation of the novel fungicide fluopyram in aqueous solution: kinetics, transformation products, and toxicity evolvement. Environ. Sci. Pollut. Res. 23, 19096–19106. https://doi.org/10.1007/s11356-016-7073-7.

El-Athman, F., Jekel, M., Putschew, A., 2019. Reaction kinetics of corrinoid-mediated deiodination of iodinated X-ray contrast media and other iodinated organic compounds. Chemosphere 234, 971–977. https://doi.org/10.1016/j.chemosphere.2019.06.135.

Farkas, R., Mireisz, T., Toumi, M., Abbaszade, G., Sztráda, N., Tóth, E., 2023. The impact of anti-inflammatory drugs on the prokaryotic community composition and selected bacterial strains based on microcosm experiments. Microorg 11, 1447. https://doi.org/10.3390/microorganisms11061447.

Feng, Y., Huang, Y., Zhan, H., Bhatt, P., Chen, S., 2020. An overview of strobilurin fungicide degradation: current status and future perspective. Front. Microbiol. 11, 309. https://doi.org/10.3389/fmicb.2020.00389.

Ferreira, L., Rosales, E., Danko, A., Sanromán, M., Pazos, M., 2016. Bacillus thuringiensis a promising bacterium for degrading emerging pollutants. Process Saf. Environ. Prot. 101, 19–26. https://doi.org/10.1016/j.psep.2015.05.003.

Foletto, V.S., Serafin, M.B., Bottega, A., da Rosa, T.F., de, S., Machado, C., Coelho, S.S., Hörner, R., 2020. Repositioning of fluoxetine and paroxetine: study of potential antibacterial activity and its combination with ciprofloxacin. Med. Chem. Res. 29, 556–563. https://doi.org/10.1007/s00044-020-02507-6.

Ghattas, A.-K., Fischer, F., Wick, A., Ternes, T., 2017. Anaerobic biodegradation of (emerging) organic contaminants in the aquatic environment. Water Res. 116, 268–295. https://doi.org/10.1016/j.watres.2017.02.001.

Gómez, R., Arce, M., Sánchez, J., del Mar Sánchez-Montoya, M., 2012. The effects of drying on sediment nitrogen content in a Mediterranean intermittent stream: a microcosms study. Hydrobiologia 679, 43–59. https://doi.org/10.1007/s10750-011-0854-6.

Gornik, T., Carena, L., Kosjek, T., Vione, D., 2021. Phototransformation study of the antidepressant paroxetine in surface waters. Sci. Total Environ. 774, 145380. https://doi.org/10.1016/j.scitotenv.2021.145380.

Gould, S., Winter, M., Norton, W., Tyler, C., 2021. The potential for adverse effects in fish exposed to antidepressants in the aquatic environment. Environ. Sci. Technol. 55, 16299–16312. https://doi.org/10.1021/acs.est.1c04724.

Höhne, A., Müller, B., Schulz, H., Dara, R., Posselt, M., Lewandowski, J., McCallum, J., 2022. Fate of trace organic compounds in the hyporheic zone: influence of microbial metabolism. Water Res. 224, 119056. https://doi.org/10.1016/j.watres.2022.119056.

Jiang, W., Zhang, M., Zhu, Q., Wu, C., Jiang, M., Ke, Z., Zhou, Y., Qiu, J., Do ng, W., Hong, Q., 2022. Esterase TriH responsible for the hydrolysis of trifloxystrobin in *Hyphomicrobium* sp. B1. Int. Biodeterior. Biodegrad. 174, 105465. https://doi.org/10.1016/j.ibiod.2022.105465.

Manasfi, R., Tadic, D., Gomez, O., Perez, S., Chiron, S., 2022. Persistence of N-oxides transformation products of tertiary amine drugs at lab and field studies. Chemosphere 309, 306661. https://doi.org/10.1016/j.chemosphere.2022.136661.

Mandaric, L., Kalogianni, E., Skoulikidis, N., Petrovic, M., Sabater, S., 2019. Contamination patterns and attenuation of pharmaceuticals in a temporary Mediterranean river. Sci. Total Environ. 647, 561–569. https://doi.org/10.1016/j.scitotenv.2018.07.308.

Marti, E., Balcazar, J.L., 2014. Use of pyrosequencing to explore the benthic bacterial community structure in a river impacted by wastewater treatment plant discharges. Res. Microbiol. 165, 468–471. https://doi.org/10.1016/j.resmic.2014.04.002.

Mekonnen, T., Panne, U., Koch, M., 2018. New photodegradation products of the fungicide fluopyram: structural elucidation and mechanism identification. Molecules 23, 2940. https://doi.org/10.3390/molecules23112940.

Meng, Z., Cui, J., Yang, C., Bao, X., Wang, J., Chen, X., 2022. Toxicity effects of chlorantraniliprole in zebrafish (Danio rerio) involving in liver function and metabolic phenotype. Pest. Biochem. Physiol. 187, 105194. https://doi.org/10.1016/j.pestbp.2022.105194.

Mueller, B., Schulz, H., Danczak, R., Putschew, A., Lewandowski, J., 2021. Simultaneous attenuation of trace organics and change in organic matter composition in the hyporheic zone of urban streams. Sci. Rep. 11, 4179. https://doi.org/10.1038/s41598-021-83750-8.

Palomo, A., Pedersen, A., Fowler, S., Dechesne, A., Sicheritz-Pontén, T., Barth, F., 2018. Comparative genomics sheds light on niche differentiation and the evolutionary history of comammox Nitrospira. ISME J. 12, 1779–1793. https://doi.org/10.1038/s41396-018-0083-3.

Perata-Maraver, I., Reiss, J., Roberton, A., 2018. Interplay of hydrology, community ecology and pollutant attenuation in the hyporheic zone. Sci. Total Environ. 610–611, 267–275. https://doi.org/10.1016/j.scitotenv.2017.08.036.

Peter, K., Herzog, S., Tian, Z., Wu, C., McCray, J., Lynch, K., Kolodziej, E., 2019. Evaluating emerging organic contaminant removal in an engineered hyporheic zone using high resolution mass spectrometry. Water Res. 150, 140–152. https://doi.org/10.1016/j.watres.2018.11.050.

Pinto, R., Weigelhofer, G., Brito, A.G., Hein, T., 2021. Effects of dry-wet cycles on nitrous oxide emissions in freshwater sediments: a synthesis. PeerJ 9, e10767. https://doi.org/10.7717/peerj.10767.

Popp, A., Weatherl, R., Moeck, C., Hollender, J., Schimer, M., 2024. Assessing hydrology, biogeochemistry, and organic micropollutants in an urban stream-aquifer system: an

interdisciplinary data set. JGR Biosciences 1, 1–10. https://doi.org/10.1029/2023JG007827.
Posselt, M., Mechelke, J., Rutere, C., Coll, C., Jaeger, A., Raza, M., Meinikmann, K., rause, S., Sobek, A., Lewandowski, J., Horn, M., Hollender, J., Benskin, J., 2020. Bacterial diversity controls transformation of wastewater-derived organic contaminants in river-simulating flumes. Environ. Sci. Technol. 54, 5467–5479. https://doi.org/10.1021/acs.est.9b06928.
Rathod, P., Shah, P., Parmar, K., Kalasariya, R.L., 2022. The fate of fluopyram in the soil–water–plant ecosystem: a review. Reviews env. Contamination 260, 1. https://doi.org/10.1007/s44169-021-00001-7.
Redman, Z., Parikh, S., Hengel, M., Tjeerdema, R., 2019. Influence of flooding, salinization, and soil properties on degradation of chlorantraniliprole in California rice field soils. J. Agric. Food Chem. 67, 8130–8137. https://doi.org/10.1021/acs.jafc.9b02947.
Reith, C.J., Spahr, S., Putschew, A., Lewandowski, J., 2023. Attenuation of trace organic compounds along hyporheic flow paths in a lowland sandbed stream. J. Hydrol. 624, 129905. https://doi.org/10.1016/j.jhydrol.2023.129905.
Romero, F., Sabater, S., Font, C., Balcazar, J.-L., Acuna, V., 2019. Desiccation events change the microbial response to gradients of wastewater effluent pollution. Water Res. 151, 371–380. https://doi.org/10.1016/j.watres.2018.12.028.
Rosman, M., Acuna, V., Petrovic, M., 2018. Effects of chronic pollution and water flow intermittency on stream biofilms biodegradation capacity. Environ. Pollut. 233, 1131–1137. https://doi.org/10.1016/j.envpol.2017.10.019.
Rutere, C., Posselt, M., Ho, A., Horn, M., 2021. Biodegradation of metoprolol in oxic and anoxic hyporheic zone sediments: unexpected effects on microbial communities. Appl. Microbiol. Biotechnol. 105, 6103–6115. https://doi.org/10.1007/s00253-021-11466-w.
Ryan, M., Pembroke, J., Adley, C., 2007. Ralstonia pickettii in environmental biotechnology: potential and applications. J. Appl. Microbiol. 103, 754–764. https://doi.org/10.1111/j.1365-2672.2007.03361.x.
Sabater-Liesa, L., Montemurro, N., Ginebra, A., Barcelo, D., Eichhorn, P., Perez, S., 2021. Retrospective mass spectrometric analysis of wastewater-fed mesocosms to assess the degradation of drugs and their human metabolites. J. Hazard Mater. 408, 124984. https://doi.org/10.1016/j.jhazmat.2020.124984.
Schaper, J., Posselt, M., McCallum, J., Banks, E., Hehne, A., Meinikmann, K., Shanafield, M., Batelaan, O., Lewandowski, J., 2018. Hyporheic exchange controls fate of trace organic compounds in an urban stream. Environ. Sci. Technol. 52, 12285–12294. https://doi.org/10.1021/acs.est.8b03117.
Schaper, J., Posselt, M., Bouchez, C., Jaeger, A., Neetzmann, G., Putschew, A., Singer, G., Lewandowki, J., 2019. Fate of trace organic compounds in the hyporheic zone: influence of retardation, the benthic biolayer, and organic carbon. Environ. Sci. Technol. 53, 4224–4234. https://doi.org/10.1021/acs.est.8b06231.
Schink, B., 2006. Microbially driven redox reactions in anoxic environments: pathways, energetics, and biochemical consequences. Eng. Life Sci. 6 (3). https://doi.org/10.1002/elsc.200620130.
Schleker, S., Rist, M., Matera, C., Damijonaitis, A., Collienne, U., Matsuoka, K., Habash, S., Twelker, K., Gutbrod, O., Saalwächter, C., Windau, M., Matthiesen, M., Stefanovka, T., Scarwey, M., Marx, M., Geibel, S., Grundler, F., 2022. Mode of action of fluopyram in plant-parasitic nematodes. Sci. Rep. 12, 11954. https://doi.org/10.1038/s41598-022-15782-7.
Schloss, P., Westcott, S., Ryabin, T., Hall, J., Hartmann, M., Hollister, E., Lesniewski, R., Oakley, B., Parks, D., Robinson, C., Sahl, J., Stres, B., Thallinger, G., Van Horn, D., Weber, C., 2009. Introducing mothur: open-source, platform-independent, community-supported software for describing and comparing microbial communities. Appl. Environ. Microbiol. 75, 7537–7541. https://doi.org/10.1128/AEM.01541-09.
Schymanski, E.L., Jeon, J., Gulde, R., Fenner, K., Ruff, M., Singer, H.P., Hollender, J., 2014. Identifying small molecules via high resolution mass spectrometry: communicating confidence. Environ. Sci. Technol. 48, 2097–2098. https://doi.org/10.1021/es5002105.
Sun, G., Zhu, Y., Saeed, T., Zhang, G., Lu, X., 2012. Nitrogen removal and microbial community profiles in six wetland columns receiving high ammonia load. Chem. Eng. J. 203, 326–332. https://doi.org/10.1016/j.cej.2012.07.052.
Tadić, D., Manasfi, R., Bertrand, M., Sauvêtre, A., Chiron, S., 2022. Use of passive and grab sampling and high-resolution mass spectrometry for non-targeted analysis of emerging contaminants and their semi-quantification in water. Molecules 27, 3167. https://doi.org/10.3390/molecules27103167.
Tomazini, R., Saia, F., van der Zaan, B., Grosseli, G., Fadini, P., de Oliveira, R., Gregoracci, G., Mozetto, A., van Vugt-Lussenburg, B., Brouwer, A., Langenhoff, A., 2021. Biodegradation of fipronil: transformation products, microbial characterisation and toxicity assessment. Water Air Soil Pollut. 232, 123. https://doi.org/10.1007/s11270-021-05071-w.
Veloso, S., Amouroux, D., Lanceleur, L., Cagnon, C., Monperrus, M., Deborde, J., Laureau, C.C., Duran, R., 2023. Keystone microbial taxa organize micropollutant-related modules shaping the microbial community structure in estuarine sediments. J. Hazard Mater. 448, 130858. https://doi.org/10.1016/j.jhazmat.2023.130858.
Venkiteshwaran, K., Milferstedt, K., Hamelin, J., Zitomer, D.H., 2016. Anaerobic digester bioaugmentation influences quasi steady state performance and microbial community. Water Res. 104, 128–136. https://doi.org/10.1016/j.watres.2016.08.012.
Völker, J., Vogt, T., Castronova, S., Wick, A., Ternes, T., Joss, A., Oehlmann, J., Wagner, M., 2017. Extended anaerobic conditions in the biological wastewater treatment: higher reduction of toxicity compared to target organic micropollutants. Water Res. 116, 220–230. https://doi.org/10.1016/j.watres.2017.03.030.
Wang, X., Li, X., Wang, Y., Qin, Y., Yan, B., Martyniuk, C., 2021. A comprehensive review of strobilurin fungicide toxicity in aquatic species: emphasis on mode of action from the zebrafish model. Environ. Pollut. 275, 116671. https://doi.org/10.1016/j.envpol.2021.116671.
Wei, P., Liu, Y., Li, W., Qian, Y., Nie, Y., Kim, D., Wang, M., 2016. Metabolic and dynamic profiling for risk assessment of fluopyram, a typical phenylamide fungicide widely applied in vegetableecosystem. Sci. Rep. 6, 33898. https://doi.org/10.1038/srep33898.
Willumsen, P.A., Johansen, J.E., Karlson, U., Hansen, B.M., 2005. Isolation and taxonomic affiliation of N-heterocyclic aromatic hydrocarbon-transforming bacteria. Appl. Microbiol. Biotechnol. 67, 420–428. https://doi.org/10.1007/s00253-004-1799-8.
Wu, M., Li, G., Chen, X., Liu, J., Liu, M., Jiang, C., Li, Z., 2018. Rational dose of insecticide chlorantraniliprole displays a transient impact on the microbial metabolic functions and bacterial community in a silty-loam paddy soil. Sci. Total Environ. 616–617, 236–244. https://doi.org/10.1016/j.scitotenv.2017.11.012.
Yadav, S., Khan, MohdA., Sharma, R., Malik, A., Sharma, S., 2021. Potential of formulated Dyadobacter jiangsuensis strain 12851 for enhanced bioremediation of chlorpyrifos contaminated soil. Ecotoxicol. Environ. Saf. 213, 112039. https://doi.org/10.1016/j.ecoenv.2021.112039.
Zeeshan, M., Schmann, P., Pabst, S., Ruhl, A., 2023. Transformation of potentially persistent and mobile organic micropollutants in column experiments. Heliyon 9, e15822. https://doi.org/10.1016/j.heliyon.2023.e15822.
Zhang, Y., Xu, J., Dong, F., Liu, X., Wu, X., Zheng, Y., 2014. Response of microbial community to a new fungicide fluopyram in the silty-loam agricultural soil. Ecotoxicol. Environ. Saf. 108, 273–280. https://doi.org/10.1016/j.ecoenv.2014.07.018.